

CRYSTALLIZATION P 127-131

Crystallization and X-ray crystallographic analysis of the C-terminal domain of *Bacillus subtilis* GabR in complex with pyridoxal 5'-phosphate and γ -aminobutyric acid

Seong Ah Park and Ki Seog Lee*

Department of Clinical Laboratory Science, College of Health Sciences, Catholic University of Pusan, Busan 46252, Republic of Korea

*Correspondence: kslee@cup.ac.kr

Bacillus subtilis GabR (BsGabR) functions as a transcriptional activator that regulates the expression of *gabTD* operon involved in the γ -aminobutyric acid (GABA) catabolism. Most studies of BsGabR have been focused on the structure-functional relationship regarding the C-terminal aminotransferase-like domain of BsGabR (BsGabR-CTD), but it still remains unclear due to lack of the structural information containing the GABA. To better understand the role of this domain, BsGabR-CTD was purified and crystallized in complex with pyridoxal 5'-phosphate and GABA. The crystal of ternary complex diffracted to a resolution of 2.0 Å and belonged to the tetragonal space group $P4_1$, with unit-cell parameters $a = b = 118.497$, $c = 75.862$ Å. Preliminary molecular replacement further confirmed the presence of one dimer in the asymmetric unit with a Matthews coefficient (V_M) of 2.86 Å³ Da⁻¹, corresponding to a solvent content of 56.9%.

INTRODUCTION

Bacterial proteins belonging to the MocR/GabR family, which are found in various bacteria, play a critical role as bacterial transcriptional regulator (El Qaidi et al., 2013; Jochmann et al., 2011; Wiethaus et al., 2008). All members of this family have a characteristic structure, as a chimeric protein incorporating an N-terminal helix-turn-helix (HTH) DNA-binding domain and the C-terminal putative aminotransferase (AT) domain (Belitsky and Sonenshein, 2002; Rigali et al., 2002). Here, the HTH-containing regions are similar to the winged HTH regions of the broad GntR family, and the C-terminal domain belongs to the well-known superfamily of fold type-I pyridoxal 5'-phosphate (PLP)-dependent enzymes, which are mainly involved in the metabolism of amino acids (Bramucci et al., 2011). Several members of this family have been studied focusing on the biochemical functions based on their structural characteristics (Belitsky and Sonenshein, 2002; Rigali et al., 2002), but the functional relationship between these domains still remains unclear. Thus, the research on the roles of each domain to understand the molecular mechanism of the chimeric MocR/GabR proteins will be intriguing and attractive.

Bacillus subtilis GabR (BsGabR) belongs to the most extensively studied MocR/GabR family, and regulates the transcription of the *gab* gene cluster that is involved in the γ -aminobutyric acid (GABA) catabolism introducing the GABA into tricarboxylic acid (TCA) cycle (Belitsky and Sonenshein, 2002). The GABA is found in a wide range of organisms (Bouche et al., 2003), and is utilized for various roles such as a signaling molecule or as a significant component

for the generation of metabolic energy (Fait et al., 2008). Namely, BsGabR serves as a negative regulator of *gabR* regardless of the presence or absence of GABA and PLP (Edayathumangalam et al., 2013). On the other hand, the BsGabR enhances the expression of enzymes in the *gabTD* operon, which are directly involved in the glutamate production from GABA, under the presence of PLP and GABA (Belitsky and Sonenshein, 2002). Under these perspectives, the transcriptional regulator GabR is able to be an attractive target for elucidating the resistance mechanism of pathogenic bacteria, which may enable to produce an alternative metabolic pathway that bypasses the action of antibiotics, such as the GABA catabolism (Aronson et al., 1975; Tenover, 2006).

Recent structural studies revealed that BsGabR consists of two domains connected by a long linker and forms a head-to-tail domain-swap homodimer in which the N-terminal HTH domain of one subunit interacts with the C-terminal aminotransferase-like (AT-like) domain of the other subunit (Edayathumangalam et al., 2013; Okuda et al., 2015). However, the structure-based information for understanding the functional details of C-terminal AT-like domain, interacting with the GABA that is required to activate the transcription of *gabTD* operon, has not yet been reported. Therefore, as the first step towards the elucidation of its structure, we have constructed the truncated BsGabR containing the C-terminal AT-like domain (BsGabR-CTD), and report the crystallization and preliminary X-ray crystallographic analysis of BsGabR-CTD in a ternary complex with the PLP and GABA as ligands.

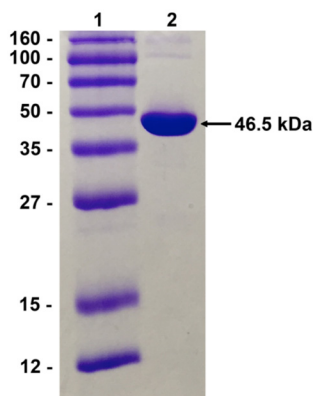


FIGURE 1 | SDS-PAGE analysis of BsGabR-CTD. Lane 1, molecular-weight markers (labelled in kDa.); lane 2, purified BsGabR-CTD protein.



FIGURE 2 | Crystal of BsGabR-CTD in complex with PLP and GABA. The ternary complex crystal dimension is approximately $0.6 \times 0.1 \times 0.1$ mm.

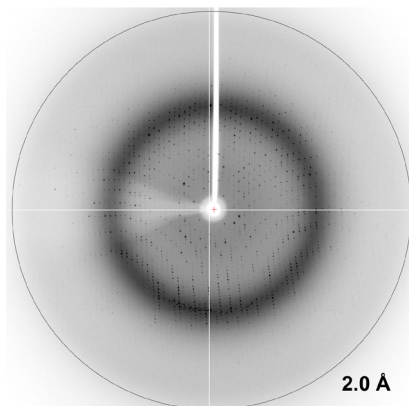


FIGURE 3 | X-ray diffraction pattern of ternary complex crystal obtained using an ADSC Quantum 270r CCD detector. A resolution circle at 2.0 Å is shown.

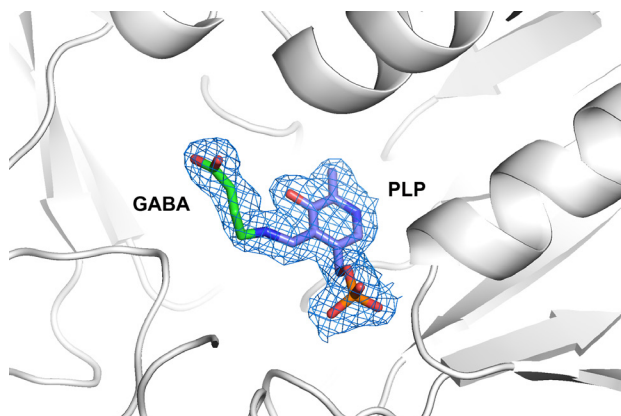


FIGURE 4 | Structure of ligand binding site of BsGabR-CTD. The location of PLP-GABA adduct is shown with an omitted $2F_o - F_c$ electron density map (blue mesh) contoured at 1.0σ . Bound ligands are represented by stick models in blue for PLP and green for GABA.

RESULTS AND DISCUSSION

The gene encoding the BsGabR-CTD from *B. subtilis* was successfully cloned into the pET-28a vector. The recombinant protein, which contains 379 amino acids with a calculated molecular weight of 46.5 kDa, was overexpressed in *Escherichia coli* BL21 (DE3), and was purified using an Ni^{2+} -chelated HiTrap Chelating HP column and gel filtration. The purified protein appeared a single band on SDS-PAGE, with estimated purity over 95% (Figure 1). The crystals of BsGabR-CTD suitable for X-ray diffraction were obtained within 7 days using an optimized reservoir solution consisting of 0.1 M HEPES, pH 7.5, 1% (w/v) polyethylene glycol 8000, and were then soaked with the PLP and GABA to form the ternary complex. The dimension of the ternary complex crystal was approximately $0.6 \times 0.1 \times 0.1$ mm (Figure 2). The crystal of BsGabR-CTD in complex with PLP and GABA readily diffracted to better than 2.0 Å resolution (Figure 3),

and was found to belong to the tetragonal space group $P4_1$, with unit-cell parameters $a = b = 118.497$, $c = 75.862$ Å. Assuming the presence of two monomers per asymmetric unit, the Matthews coefficient V_M value was calculated to be $2.86 \text{ \AA}^3 \text{ Da}^{-1}$, with estimated solvent content of 56.9% (Kantardjieff and Rupp, 2003; Matthews, 1968).

Structure determination was attempted by molecular replacement using *MOLREP* program (Vagin and Teplyakov, 2010) in the *CCP4* (Winn et al., 2011) with the crystal structure of apo-BsGabR (PDB entry 4MGR) (Edayathumangalam et al., 2013) as a search model. As expected, the results of molecular replacement indicated two monomers corresponding to a noncrystallographic dimer of BsGabR-CTD in the asymmetric unit. After rigid body and several restrained refinement by the program *PHENIX* (Adams et al., 2010), the values of R_{factor} and R_{free} were approximately 31% and 35%, respectively. However,

TABLE 1 | Macromolecule-production information

Source organism	<i>B. subtilis</i>
DNA source	Genomic DNA
Forward primer*	5'-ATA <u>GGA TCC</u> ATG GAG ATT CAC ATC GAC CAG-3'
Reverse primer*	5'-ATA <u>CTC GAG</u> TCA ATC CCC TGT AAC GGG GAT-3'
Cloning vector	pET-28a
Expression vector	pET-28a
Expression host	<i>E. coli</i> BL21 (DE3)
Complete amino-acid sequence of the construct produced**	<u>MGSSHHHHHHSSGLVPRGSH</u> MEIHIDQSDWISFSHMSSDTHDFPIKSWFRCEQKAASRSYRTLGDMSHPQGIYEVRAAITRLISLTRGVKCRPEQMIIGAGTQVLMQLLTELPEAVYAMEEPGYRRMYQLLKNA GKQVKTIMLDEKGMISIAEITRQQPDVLVTPSHQFPGSGTIMPVSRRIQLLNWAAEPRRYIIEDDDYDSEF TYDVSIPALQSLDRFQNVIMGTFSKSLPGLRISYMLPPELLRAYKQRGYDLQTCSSSLQTLTQEFIE SGEYQKHIKKMKQHYKEKRERLITALEAEFSGEVTVKGANAGLHFVTEFDTRRTEQDILSHAAGLQLEIF GMSRFNLKENKRQTGRPALIIGFARLKEEIQEGVQRLFKAVYGHKKIPVTGD

* Restriction enzyme sites are underlined.

** The extra amino acids introduced into the wild-type BsGabR-CTD protein by cloning are underlined.

TABLE 2 | Crystallization condition.

Method	Vapour diffusion in hanging drops
Plate type	24-well XRL plate (Molecular Dimensions)
Temperature (K)	294
Protein concentration (mg ml ⁻¹)	6.5
Buffer composition of protein solution	30 mM Tris-HCl, pH 8.5, 150 mM NaCl, 2 mM DTT, 10% glycerol
Composition of reservoir solution	0.1 M HEPES, pH 7.5, 1–1.5% (w/v) polyethylene glycol 8000
Volume and ratio of drop*	2 µl, 1:1
Volume of reservoir (µl)	500

* The volume ratio is that of protein : reservoir.

further refinement could not lead the R_{free} value to be below 30%, although the electron-density map showed a good consistency with the model structure. To solve this problem, we **carried out** the analysis of diffraction data using the program of *phenix.xtriage* (Adams et al., 2010). The crystal in a ternary complex revealed to be a merohedral twin, indicating a twin fraction of 0.29 and a twin law ($h, -k, -l$). Recently, we have confirmed the presence of PLP and GABA located in the ligand-binding site of BsGabR-CTD, based on the omitted $2F_o - F_c$ electron density map contoured at 1.0σ (Figure 4). Further refinements of the model structure are currently in progress, and a detailed description of the ternary complex structure of BsGabR-CTD will be reported elsewhere.

TABLE 3 | Data-collection statistics. Values in parentheses are for the outer shell.

	BsGabR-CTD- PLP-GABA complex
Diffraction source	Beamline 7A, PAL
Wavelength (Å)	1.0000
Temperature (K)	100
Detector	ADSC Quantum 270r CCD
Crystal-to-detector distance (mm)	240
Rotation range per image (°)	0.5
Total rotation range (°)	180
Exposure time per image (s)	1
Space group	P41
Unit-cell parameters (Å, °)	$a = 118.497, b = 118.497, c = 75.862$ $\alpha = \beta = \gamma = 90$
Mosaicity (°)	0.53
Resolution range (Å)	50.5 – 2.0 (2.07 – 2.00)
Total No. of reflections	69052
No. of unique reflections	6399
Completeness (%)	96.5 (89.7)
Multiplicity	4.6 (2.5)
$\langle I/\sigma(I) \rangle$	14.6 (3.0)
R_{merge} (%)	8.7 (29.6)
Overall B factor from Wilson plot (Å ²)	20.97

* $R_{\text{merge}} = \sum_{hkl} |I_{hkl}| - \langle I_{hkl} \rangle / \sum_{hkl} I_{hkl}$, where I represents the observed intensity, $\langle I \rangle$ represents the average intensity, and i counts through all symmetry-related reflections.

METHODS

Protein expression and purification

The BsGabR-CTD gene was amplified from *B. subtilis* genomic DNA by polymerase chain reaction (PCR) using the forward and reverse primers. The primers contained modification to add appropriate restriction endonuclease for insertion into the vector, where *Bam*HI site in the forward primer and the *Xho*I site in the reverse primer are underlined in Table 1. The PCR-amplified DNA fragment was then digested with *Bam*HI and *Xho*I and inserted into the bacterial expression vector pET-28a (Novagen, USA) to generate the plasmid pBsGabR-CTD consisting of BsGabR-CTD with six consecutive histidines at the N-terminus. *E. coli* BL21 (DE3) cells (Novagen, USA) harbouring pBsGabR-CTD were grown in Luria-Bertani medium with 50 µg ml⁻¹ kanamycin at 25°C to an optical density at 600 nm of 0.6. Protein expression was induced by addition of 0.5 mM isopropyl-β-D-1-thiogalactopyranoside and incubation at 18°C for a further 18 h. The cells were harvested by centrifugation at 5000 g for 30 min at 4°C.

The harvested cell pellets were suspended in buffer A (30 mM Tris-HCl, pH 8.5, 500 mM NaCl, 5 mM β-mercaptoethanol (βME), 10% glycerol) containing 1 mM phenylmethylsulfonyl fluoride and disrupted by sonication at 4°C. The crude lysate was centrifuged at 25000 g for 30 min at 4°C. The supernatant was loaded onto a Ni²⁺-chelated HiTrap chelating HP column (GE Healthcare, USA) equilibrated in buffer A. The bound protein was eluted with a linear gradient of buffer B (30 mM Tris-HCl, pH 8.5, 500 mM NaCl, 5 mM βME, 10% glycerol, 500 mM imidazole). Fractions containing BsGabR-CTD were identified by SDS-PAGE and subsequently purified by gel-filtration chromatography on a HiLoad 16/60 Superdex 200 column (GE Healthcare, USA), which had been equilibrated with gel buffer (30 mM Tris-HCl pH 8.5, 150mM NaCl, 2 mM dithiothreitol, 10% glycerol). The soluble fractions containing protein were pooled together and concentrated to 6.5 mg/ml using an Amicon Ultra-15 centrifugal filter device (Millipore, USA).

Protein crystallization

Preliminary crystallization screening for the BsGabR-CTD was performed via the hanging drop vapour-diffusion method (0.2 µl protein solution and 0.2 µl reservoir solution equilibrated against 70 µl reservoir solution) using various commercial screening kits (Crystal Screen, Crystal Screen 2, PEGRx 1 and 2 from Hampton Research, USA and Wizard I, II, III and IV from Emerald Biosystems, USA) in 96-well microplates at 21°C. Initial crystals were obtained using the following condition: 0.1 M HEPES, pH 7.5, 4% (w/v) polyethylene glycol 8000 (from PEGRx 1; Hampton Research, USA). Crystal growth was optimized using the hanging-drop vapour diffusion method in 24-well XRL plates (Molecular Dimensions, UK); each drop was made up of 1 µl protein solution and 1 µl reservoir solution [0.1 M HEPES, pH 7.5, 1–1.5% (w/v) polyethylene glycol 8000] and was equilibrated over 500 µl reservoir solution (Table 2). The crystal of BsGabR-CTD in a ternary complex with PLP and GABA was obtained by soaking the native crystals in the reservoir solution containing 1 mM PLP and 10–30 mM GABA for over 3h at 21°C.

Data collection and processing

For data collection of the crystal in cryogenic condition, all crystals were transferred into a cryoprotection solution consisting of 30% ethylene glycol in reservoir solution. The cryoprotected crystals were then directly flash-cooled at -180°C in a stream of nitrogen gas. The diffraction data sets were collected on beamline 7A at the Pohang Light Source (Pohang, South Korea) using an ADSC Quantum 270r CCD detector. A total range of 180° was covered with an oscillation angle of 0.5° and 1 s exposure per frame. The distance from the crystal to the detector was 240 mm. The X-ray diffraction data showed that the ternary complex crystal diffracted to 2.0 Å resolution. All data sets were indexed, integrated and scaled using the *HKL-2000* software package (Otwinowski and Minor, 1997). Detailed information on data collection is given in Table 3.

CONFLICT OF INTEREST

The authors declare that they have no conflict of interest.

ACKNOWLEDGEMENTS

We would like to thank the staff of beamline 7A at the Pohang Accelerator Laboratory in South Korea for their assistance during X-ray data collection.

Original Submission: Oct 20, 2017

Revised Version Received: Oct 26, 2017

Accepted: Oct 27, 2017

REFERENCES

- Adams, P.D., Afonine, P.V., Bunkoczi, G., Chen, V.B., Davis, I.W., Echols, N., Headd, J.J., Hung, L.W., Kapral, G.J., Grosse-Kunstleve, R.W., McCoy, A.J., Moriarty, N.W., Oeffner, R., Read, R.J., Richardson, D.C., *et al.* (2010). PHENIX: a comprehensive Python-based system for macromolecular structure solution. *Acta Crystallogr D Biol Crystallogr* **66**, 213–221.
- Aronson, J.N., Borris, D.P., Doerner, J.F., and Akers, E. (1975). Gamma-aminobutyric acid pathway and modified tricarboxylic acid cycle activity during growth and sporulation of *Bacillus thuringiensis*. *Appl Microbiol* **30**, 489–492.
- Belitsky, B.R., and Sonenshein, A.L. (2002). GabR, a member of a novel protein family, regulates the utilization of gamma-aminobutyrate in *Bacillus subtilis*. *Mol Microbiol* **45**, 569–583.
- Bouche, N., Fait, A., Bouchez, D., Moller, S.G., and Fromm, H. (2003). Mitochondrial succinic semialdehyde dehydrogenase of the gamma-aminobutyrate shunt is required to restrict levels of reactive oxygen intermediates in plants. *Proc Natl Acad Sci U S A* **100**, 6843–6848.
- Bramucci, E., Milano, T., and Pascarella, S. (2011). Genomic distribution and heterogeneity of MocR-like transcriptional factors containing a domain belonging to the superfamily of the pyridoxal-5'-phosphate dependent enzymes of fold type I. *Biochem Biophys Res Commun* **415**, 88–93.
- Edayathumangalam, R., Wu, R., Garcia, R., Wang, Y., Wang, W., Kreinbring, C.A., Bach, A., Liao, J., Stone, T.A., Terwilliger, T.C., Hoang, Q.Q., Belitsky, B.R., Petsko, G.A., Ringe, D., and Liu, D. (2013). Crystal structure of *Bacillus subtilis* GabR, an autorepressor and transcriptional activator of *gabT*. *Proc Natl Acad Sci U S A* **110**, 17820–17825.
- El Qaidi, S., Yang, J., Zhang, J.R., Metzger, D.W., and Bai, G. (2013). The vitamin B(6) biosynthesis pathway in *Streptococcus pneumoniae* is controlled by pyridoxal 5'-phosphate and the transcription factor PdxR and has an impact on ear infection. *J Bacteriol* **195**, 2187–2196.
- Fait, A., Fromm, H., Walter, D., Galili, G., and Fernie, A.R. (2008). Highway or byway: the metabolic role of the GABA shunt in plants. *Trends Plant Sci* **13**, 14–19.
- Jochmann, N., Gotker, S., and Tauch, A. (2011). Positive transcriptional control of the pyridoxal phosphate biosynthesis genes *pdxST* by the MocR-type regulator PdxR of *Corynebacterium glutamicum* ATCC 13032. *Microbiology* **157**, 77–88.
- Kantardjiev, K.A., and Rupp, B. (2003). Matthews coefficient probabilities: Improved estimates for unit cell contents of proteins, DNA, and protein-nucleic acid complex crystals. *Protein Sci* **12**, 1865–1871.
- Matthews, B.W. (1968). Solvent content of protein crystals. *J Mol Biol* **33**, 491–497.
- Okuda, K., Kato, S., Ito, T., Shiraki, S., Kawase, Y., Goto, M., Kawashima, S., Hemmi, H., Fukada, H., and Yoshimura, T. (2015). Role of the aminotransferase domain in *Bacillus subtilis* GabR, a pyridoxal 5'-phosphate-dependent transcriptional regulator. *Mol Microbiol* **95**, 245–257.
- Otwinowski, Z., and Minor, W. (1997). Processing of X-ray diffraction data collected in oscillation mode. *Methods Enzymol* **276**, 307–326.
- Rigali, S., Derouaux, A., Giannotta, F., and Dusart, J. (2002). Subdivision of the helix-turn-helix GntR family of bacterial regulators in the FadR, HutC, MocR, and YtrA subfamilies. *J Biol Chem* **277**, 12507–12515.
- Tenover, F.C. (2006). Mechanisms of antimicrobial resistance in bacteria. *Am J Med* **119**, S3–10; discussion S62–70.

Vagin, A., and Teplyakov, A. (2010). Molecular replacement with MOLREP. *Acta Crystallogr D Biol Crystallogr* **66**, 22-25.

Wiethaus, J., Schubert, B., Pfander, Y., Narberhaus, F., and Masepohl, B. (2008). The GntR-like regulator TauR activates expression of taurine utilization genes in *Rhodobacter capsulatus*. *J Bacteriol* **190**, 487-493.

Winn, M.D., Ballard, C.C., Cowtan, K.D., Dodson, E.J., Emsley, P., Evans, P.R., Keegan, R.M., Krissinel, E.B., Leslie, A.G., McCoy, A., McNicholas, S.J., Murshudov, G.N., Pannu, N.S., Potterton, E.A., Powell, H.R., *et al.* (2011). Overview of the CCP4 suite and current developments. *Acta Crystallogr D Biol Crystallogr* **67**, 235-242.